Eur Biophys J (1987) 15:87–102

European Biophysics Journal

Order and fluidity of lipid membranes as determined by fluorescence anisotropy decay

L. Best*, E. John, and F. Jähnig

Max-Planck-Institut für Biologie, Corrensstrasse 38, D-7400 Tübingen, Federal Republic of Germany

Received June 23, 1986/Accepted in revised form December 23, 1986

Abstract. The fluorescence anisotropy decay of four different probes in bilayers of dimyristoylphosphatidylcholine was measured. The probes are diphenylhexatriene, diphenyloctatetraene, trimethylaminodiphenylhexatriene, and *trans*-parinaric acid. The data for each probe were analyzed in terms of two orientational order parameters, the ordinary order parameter and a higher one, and two rotational diffusion coefficients. The order parameters are largely independent of probe size, but depend on the position of the probes along the membrane normal, thus reflecting the profile of lipid order. If a probe is located in the plateau region of lipid order, its order parameters are interpreted as representing the rigid-body order of lipids. According to this interpretation, the total lipid order in the plateau region originates about equally from rigid-body order and conformational order. The two order parameters obtained for each probe are used to derive approximate angular distributions of the probe molecules. The diffusion coefficient for rotation about the long molecular axis is found to be infinitely large, indicating unhindered rotation about this axis. The diffusion coefficient for rotation about the short molecular axes is evaluated for a viscosity which results as 0.2 poise. This viscosity for rotational diffusion is an order of magnitude smaller than the viscosity for lateral diffusion indicating that at least two viscosities are required to characterize the fluidity of a lipid membrane.

Key words: Lipid bilayers, fluorescence probes, order parameters, diffusion coefficients, viscosity

Introduction

Lipid molecules in membranes exhibit orientational order: On the average they are oriented parallel to a preferred axis, usually the membrane normal. About this preferred axis they undergo orientational fluctuations. The average orientation along a preferred axis originates in the molecular interactions which give rise to an ordering potential, the fluctuations are of thermal origin. A description of this state is given by the angular distribution of the molecular orientation. This distribution has a peak at the orientation corresponding to the preferred axis. The more pronounced the peak, the stronger is the orientational order. The angular distribution cannot be measured directly, only averages over the distribution are detectable such as the order parameters $\langle P_i \rangle$ with P_i denoting the Legendre polynomials. $\langle P_2 \rangle$ is the ordinary order parameter often denoted as S, and $\langle P_4 \rangle$, $\langle P_6 \rangle$, ... are higher order parameters.

A complete description of membranes includes the kinetics of orientational order. These kinetics reflect the relaxation of an arbitrary initial distribution to the equilibrium distribution and may be described by one or more relaxation times. The relaxation times depend on the rotational diffusion coefficients of the molecules about their long and short axes and on the ordering potential in which they move. The influence of the ordering potential may be expressed in terms of the order parameters. From the diffusion coefficients one can derive, in a hydrodynamic model, two viscosities, one for rotation about the long axis and one for rotation about the short axes. These viscosities need not be equal, because the membrane is an anisotropic medium.

* Present address: Die Holzwerkstatt, Gartenstrasse 29, D-6112 Groß-Zimmern, Federal Republic of Germany

Abbreviations: FAD, fluorescence anisotropy decay; DMR, deuterium magnetic resonance; ESR, electron spin resonance; DMPC, dimyristoylphosphatidylcholine; DPPC, dipalmitoylphosphatidylcholine; DPH, 1,6-diphenyl-1,3,5-hexatriene; DPO, 1,6-diphenyl-1,3,5,7-octatetraene; TMA-DPH, 1-[4-(trimethylamino)phenyl]-6-phenyl-1,3,5-hexatriene; tPnA, *trans*-parinaric acid; NPN, *N*-phenyl-1-naphthylamine; BBO, 2,5-*bis*(4-biphenylyl)oxazole

The fluidity of a membrane may be specified as the inverse of the viscosity. If more than one viscosity exists, the fluidity involves more than one inverse viscosity.

One of the extensively used techniques to study the order and fluidity of membranes is fluorescence anisotropy decay (FAD) of probe molecules (for a review see Kinosita et al. 1984). Two kinds of information are obtained from such measurements: The residual anisotropy at long times can be evaluated for the probe order parameter $\langle P_2 \rangle$ (Heyn 1979; Jähnig 1979a; Szabo 1980), and the anisotropy decay yields the relaxation times of orientational order (Kinosita et al. 1977). Recently, the fluorescence anisotropy decay has been calculated for the case of rotational diffusion of symmetric ellipsoids in an ordering potential and was found to be given by 9 relaxation terms (Zannoni 1981; Arcioni and Zannoni 1984; van der Meer et al. 1984). The relaxation times were expressed as functions of the two diffusion coefficients for rotation about the long and short molecular axes and the two order parameters $\langle P_2 \rangle$ and $\langle P_4 \rangle$. From these order parameters an approximate form of the angular distribution of the molecules may be derived. The two diffusion coefficients, on the other hand, can be evaluated for the two viscosities for rotation about axes parallel and perpendicular to the membrane normal.

Thus, evaluation of FAD measurements in terms of probe order parameters and diffusion coefficients or viscosities is straightforward. Less clear is how probe order and diffusion is ultimately related to lipid order and diffusion. Fluorescence probes are usually rigid molecules compared to the flexible hydrocarbon chains of lipids and, therefore, may not undergo the same fluctuations as lipid chains. Lipid chain fluctuations are a superposition of rigid-body motion and conformational transitions (Petersen and Chan 1977; van der Ploeg and Berendsen 1983). The rigid-body order, by definition, is constant along the chains, whereas the conformational order decreases towards the chain ends leading to a decrease of total order along the chains, as detected by deuterium magnetic resonance (DMR) (Seelig and Seelig 1974). Rigid fluorescence probes of length comparable to that of lipid chains should, therefore, predominantly reflect the rigid-body order of lipids (Jähnig et al. 1982). If smaller probes, which adopt different positions along the membrane normal, are employed they should differ in their order parameters, thus reflecting the profile of lipid order. Analogous arguments hold for the comparison of lipid and probe diffusion where in addition differences in size may play a role.

In order to clarify some of the open questions in the relation between lipid and probe order and diffusion, we performed FAD measurements on four different probes in bilayers of dimyristoylphosphatidylcholine (DMPC): Diphenylhexatriene (DPH), diphenyloctatetraene (DPO) which differs from DPH in size by being slightly longer, trimethylamino-DPH (TMA-DPH) whose position differs from that of DPH by being shifted closer to the lipid polar heads due to the charged moiety, and *trans*-parinaric acid (tPnA) whose fluorophore presumably has a position similar to that of DPH but is attached to a flexible chain.

Except for DPO, these probes have already been investigated by other groups to different extents and often with somewhat contradictory results. Even for the most extensively employed probe, DPH, the reported data are not consistent. Three groups observed a finite residual anisotropy r_∞ (Kawato et al. 1977; Lakowicz et al. 1979, 1985; Ameloot et al. 1984), but two others did not (Chen et al. 1977; Thulborn and Beddard 1982). Furthermore, no consensus has been reached as to the relaxation times in the ordered lipid phase. TMA-DPH has been studied by one group but relaxation times have not been reported (Prendergast et al. 1981). The data on relaxation times of tPnA are also limited (Wolber and Hudson 1981). To complete the list of probes studied up to now by FAD, work on a lipid analogue of tPnA (Wolber and Hudson 1981) and on an anthroyl-labelled fatty acid (Thulborn and Beddard 1982) should be mentioned. Only in one case, namely that of DPH, has the data analysis been performed on the basis of rotational diffusion of ellipsoids in an ordering potential (Ameloot et al. 1984).

Our measurements were carried out with a pulsed laser as light source and single-photon counting electronics for detection. Such systems have already been employed for FAD measurements (Visser and van Hoek 1979; Robbins et al. 1980; Wijnaendts van Resandt and de Maeyer 1981; Lampert et al. 1983), but have not yet been applied to study order and diffusion in lipid membranes, except for one case (Thulborn and Beddard 1982).

Materials and methods

Materials

The substances used as fluorescence standards were 2,5-*bis*(4-biphenylyl)oxazole (BBO) from EGA-Chemie (Steinheim, BRD) and *N*-phenyl-1-naphthylamine (NPN) from Eastman-Kodak. DPH and DPO were purchased from EGA-Chemie, TMA-DPH from Molecular Probes (Plano, USA), and tPnA from Calbiochem (La Jolla, USA). NPN and

DPO were recrystallized from methanol and chloroform, respectively, the other substances were used without further purification. Glycerol (grade pA) was from Serva, paraffin (spectroscopic grade) and cyclohexane (spectroscopic grade) from Merck, and DMPC from Fluka.

Preparation of samples

To measure the intensity decay of fluorescence standards a $5 \cdot 10^{-6} M$ solution of NPN and a $10^{-6} M$ solution of BBO in cyclohexane were used.

Of the four FA probes the following stock solutions were prepared: $0.4 \cdot 10^{-3} M$ DPH in dioxan, $0.5 \cdot 10^{-3} M$ TMA-DPH in dimethylsulfoxide, $10^{-3} M$ DPO in dioxan, and $0.5 \cdot 10^{-3} M$ tPnA with 10% (mol/mol) butylated hydroxytoluene in ethanol. For FAD measurements in glycerol and paraffin, sufficient stock solution was added to obtain the following final concentrations: $4 \cdot 10^{-6} M$ DPH, $5 \cdot 10^{-6} M$ TMA-DPH, $8 \cdot 10^{-6} M$ DPO, and $3 \cdot 10^{-6} M$ tPnA in glycerol and $3 \cdot 10^{-6} M$ DPH in paraffin. Control samples were prepared by adding appropriate amounts of solvent to glycerol or paraffin.

For FAD measurements on lipid membranes, DMPC and sufficient stock solution were mixed in methanol. After rotary-evaporation and drying in vacuo, buffer ($5 \cdot 10^{-2} M$ potassium-hydrogen phosphate, $10^{-4} M$ EDTA, pH 6.5) was added. The suspension was vortexed for 5 min and then incubated for 60 min at 38 °C and for several hours at 6 °C. The sample with tPnA was protected from light and oxygen during the preparation. The final concentration of DMPC was $2-4 \cdot 10^{-4} M$, the molar ratios of lipid to fluorophores were 250 for DPO and 500–1,000 for DPH, TMA-DPH, and tPnA. Control samples were prepared in the same way except for the addition of fluorophores.

Fluorescence measurements

For each measurement four data sets from the following samples must be recorded: The fluorescence sample, the control sample, the fluorescence standard sample, and the fluorescence standard control sample. The intensity of a fluorescence sample was typically 20 times higher than that of a control sample. Excitation and emission wavelengths were 333 and 430 nm, respectively, for DPH and TMA-DPH, 330 and 500 nm for DPO, 320 and 410 nm for tPnA. All samples were stirred continuously. The measurements on lipid membranes were carried out at different temperatures with equilibration for 15 min at each temperature.

Fluorescence apparatus

The temporal decay of polarized fluorescence light was detected employing a pulsed laser for excitation and single-photon counting electronics for detection. A mode-locked Ar^+ laser (Spectra Physics, model 171) pumps a dye laser (Spectra Physics, model 375) in whose resonator a cavity dumper (Spectra Physics, model 366) is inserted to generate light pulses of less than 100 ps duration at a repetition rate of 4 MHz. Using rhodamine 101 as dye, the wavelength of the light can be varied between 620 and 680 nm so that, after frequency doubling with a KDP crystal (Gsänger, Gräfelfing, BRD), monochromatic excitation between 310 and 340 nm is possible. The laser light is linearly polarized, but in order to vary the direction of polarization a Fresnel rhombus is inserted into the light path followed by a Glan prism polarizer to assure a high degree of polarization (both Halle, Berlin).

The sample holder can be rotated to bring four different 1×1 cm quartz cuvettes into the light beam. The cuvettes can be thermostated and stirred magnetically.

The emitted light is detected at right angles to the exciting light. An $f/1.7$ lens projects the illuminated volume of the sample on the entrance slit of a monochromator (ISA, model 1061). The polarization of the detected light is selected by means of a sheet polarizer (Käsemann, Oberaudorf, BRD, model Ks-W 78) and can be rotated between polarization parallel and perpendicular to the polarization of the exciting light by rotating the sheet polarizer via a stroke magnet. The photomultiplier (Philips, XP 2020 Q) is run at 2.7 kV. Its anode is connected to a constant fraction discriminator (Canberra, 1428 A) which provides the start signal for the time-to-amplitude converter (EG & G, model 457). The stop signal is generated by a portion of the exciting light pulse detected by a silicon avalanche photodiode (Telefunken, model BPW 28 A). Its electric signal is formed by a constant fraction discriminator (Elscint, model FD-N-2) before entering the time-to-amplitude converter. A multi-channel analyzer (EG & G, model IT-5300) is used for data collection.

The two components $i_{\parallel}$ and $i_{\perp}$ of the fluorescence intensity are obtained under initial polarization perpendicular to the scattering plane and final polarization parallel or perpendicular to it. They are measured alternately several times and collected in the two halves of the multichannel analyzer, each consisting of 512 data points. A typical measuring time is 10×20 s for each component. A micro computer (Kontron, model PSI 80) controls the stroke magnet for detection of $i_{\parallel}$ and $i_{\perp}$ and the multichannel

analyzer for collection of $i_\parallel$ or $i_\perp$. A faster computer (IBM, AT2) is used for data analysis.

The apparatus response function measured through light scattering from a membrane suspension is shown in Fig. 1 for $\lambda_{ex} = \lambda_{em} = 320$ nm. The full width at half maximum is 350 ps. Also shown is the anisotropy of light scattering, which turned out to be independent of time indicating that the apparatus function is identical for $i_\parallel$ and $i_\perp$.

Data analysis

From the data for $i_\parallel(t)$ and $i_\perp(t)$ of the fluorescence sample and for $i_{\parallel B}(t)$ and $i_{\perp B}(t)$ of the control (or blank) sample the total intensity (or sum) $s(t)$ and the difference $d(t)$ are derived together with their standard deviations $\sigma_s(t)$ and $\sigma_d(t)$:

$$\begin{aligned} s(t) &= [i_\parallel(t) - \gamma i_{\parallel B}(t)] + 2\beta[i_\perp(t) - \gamma i_{\perp B}(t)] \\ d(t) &= [i_\parallel(t) - \gamma i_{\parallel B}(t)] - \beta[i_\perp(t) - \gamma i_{\perp B}(t)] \\ \sigma_s^2(t) &= [i_\parallel(t) + \gamma^2 i_{\parallel B}(t)] + 4\beta^2[i_\perp(t) + \gamma^2 i_{\perp B}(t)] \\ \sigma_d^2(t) &= [i_\parallel(t) + \gamma^2 i_{\parallel B}(t)] + \beta^2[i_\perp(t) + \gamma^2 i_{\perp B}(t)] . \end{aligned} \tag{1}$$

The factor γ results from different measuring times for the fluorescence sample and the control sample. The factor β accounts for the polarization dependence of the monochromator and is determined by measuring the fluorescence intensities for the two final polarizations with the initial polarization parallel to the scattering plane. A typical value for β is 1.2. From $s(t)$ and $d(t)$ the experimental anisotropy, $r(t)$, follows as

$$r(t) = d(t)/s(t) . \tag{2}$$

The true decay laws of the fluorescence sum, difference, and anisotropy are denoted $S(t)$, $D(t)$, and $R(t)$, respectively. $S(t)$ and $R(t)$ are assumed to be given by a sum of exponential functions

$$\begin{aligned} S(t) &= \sum_{i=1}^{N} a_i \, e^{-t/\tau_i} \\ R(t) &= \sum_{i=1}^{M} b_i \, e^{-t/\phi_i} + R_\infty \end{aligned} \tag{3}$$

with $R(t)$ containing in addition a constant term, R_∞. The partial amplitudes α_i of the sum, the average life time $\bar{\tau}$, the average relaxation time $\bar{\phi}$, and the initial anisotropy R_0 are derived as

$$\begin{aligned} \alpha_i &= a_i / \sum_{i=1}^{N} a_i \\ \bar{\tau} &= \sum_{i=1}^{N} \alpha_i \tau_i \\ \bar{\phi} &= \sum_{i=1}^{M} b_i \phi_i / \sum_{i=1}^{M} b_i \\ R_0 &= \sum_{i=1}^{M} b_i + R_\infty . \end{aligned} \tag{4}$$

Convolution of the functions $S(t)$ and $D(t) = S(t) \cdot R(t)$ with the apparatus response function $p(t)$ yields the calculated curves $s_c(t)$ and $d_c(t)$ as

$$x_c(t) = \int_0^t p(t') \, X(t-t') \, dt' \qquad (x = s \text{ or } d, \; X = S \text{ or } D) , \tag{5}$$

which are to be fitted to the experimental curves $s(t)$ and $d(t)$. The difference instead of the anisotropy is fitted, because fitting $d(t)$ is simpler than $r(t)$. The same apparatus function can be used for $S(t)$ and $D(t)$, because, as shown above, $p(t)$ is independent of polarization.

Routinely, the use of an apparatus function was avoided by employing a fluorescence standard. This procedure has been introduced by Wahl et al. (1974) and elaborated by several groups (Wahl 1979; Wijnaendts van Resandt et al. 1982; Libertini and Small 1984; Zuker et al. 1985; Löfroth 1985; Kolber and Barkley 1986; van den Zegel et al. 1986). The standard has a strict mono-exponential decay with a known life time, τ_s. The total intensity $f(t) = f_\parallel(t) + 2\beta f_\perp(t)$ of the standard is measured under the final polarization at the magic angle of 54.7° relative to the initial polarization. The function $f(t)$ is set equal to the convolution of $F(t) = F(0) \, e^{-t/\tau_s}$ with the apparatus function:

$$f(t) = \int_0^t p(t') \, F(t-t') \, dt' .$$

Differentiation leads to the relation

$$\frac{\partial}{\partial t} f(t) = p(t) \, F(0) - \frac{1}{\tau_s} \int_0^t p(t') \, F(t-t') \, dt'$$

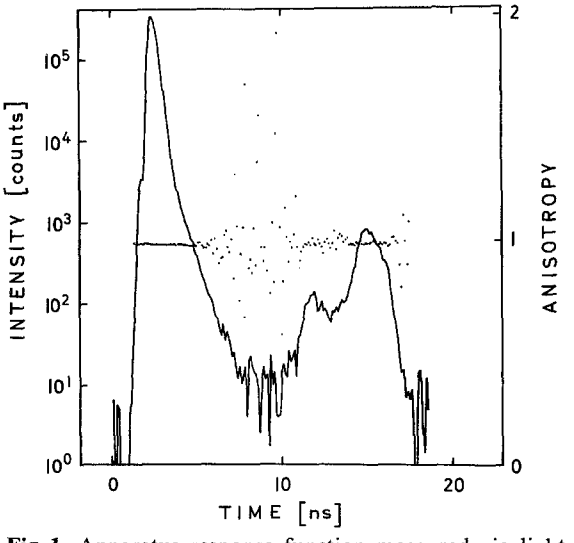

Fig. 1. Apparatus response function measured via light scattering at a dispersion of DMPC bilayers at 320 nm. The total intensity (——) and anisotropy (···) are shown

which can be transformed into an expression for the response function

$$p(t) = \frac{1}{F(0)}\left[\frac{1}{\tau_s}\int_0^t p(t')\,F(t-t')\,dt' + \frac{\partial}{\partial t}f(t)\right].$$

Insertion of this expression into Eq. (5) yields

$$x_c(t) = \frac{X(0)}{F(0)}\left[f(t) + \left(\frac{1}{\tau_s} - \frac{1}{\tau}\right)\int_0^t f(t')\frac{X(t-t')}{X(0)}\,dt'\right]. \tag{6}$$

Here we have assumed that $X(t)$ is mono-exponential, but generalization to the case of more exponential functions is straightforward (Wahl 1979). To arrive at a recurrence formula the integral in Eq. (6) is split up into two parts (Wahl 1975)

$$\int_0^t f(t')\frac{X(t-t')}{X(0)}\,dt' = \int_0^{t-t_0} f(t')\frac{X(t-t_0-t')}{X(0)}\,dt'\cdot e^{-t_0/\tau} + \int_{t-t_0}^{t} f(t')\frac{X(t-t')}{X(0)}\,dt'$$

the first part of which can be expressed in terms of $x_c(t-t_0)$ with t_0 denoting the time interval between two data points, so that

$$x_c(t) = e^{-t_0/\tau}x_c(t-t_0) + \frac{X(0)}{F(0)}\left[f(t) - e^{-t_0/\tau}f(t-t_0) + \left(\frac{1}{\tau_s} - \frac{1}{\tau}\right)\int_{t-t_0}^{t} f(t')\frac{X(t-t')}{X(0)}\,dt'\right]. \tag{7}$$

To get an estimate for the residual integral, $f(t')$ may be linearized in t'

$$f(t') = f(t-t_0) + \frac{f(t)-f(t-t_0)}{t_0}(t'-t+t_0)$$

leading to the final result

$$x_c(t) = e^{-t_0/\tau}x_c(t-t_0) + \frac{X(0)}{F(0)}[\mu_1 f(t) + \mu_2 f(t-t_0)] \tag{8}$$

with the abbreviations

$$\mu_1 = \frac{\tau}{\tau_s} + \frac{\tau}{t_0}\left(1-\frac{\tau}{\tau_s}\right)(1-e^{-t_0/\tau})$$

and

$$\mu_2 = \frac{\tau}{\tau_s}e^{-t_0/\tau} + \frac{\tau}{t_0}\left(1-\frac{\tau}{\tau_s}\right)(1-e^{-t_0/\tau}).$$

In the fit procedure, the unknown parameters a_i and τ_i of the sum and b_i, ϕ_i, and R_∞ of the anisotropy are determined by minimization of the quantities

$$\chi_x^2 = \frac{1}{n'-n}\sum_{\nu=n}^{n'} \mathrm{res}_x^2(t_\nu) \tag{9}$$

using an iteration method (Bevington 1969). The channel numbers n and n' specify the time window chosen for the fit. The residuals res_x are defined as

$$\mathrm{res}_x(t_\nu) = [x(t_\nu) - x_c(t_\nu)]/\sigma_x(t_\nu). \tag{10}$$

Here the assumption has been made that the life time τ_s of the standard is small compared to the average life time $\bar{\tau}$ of the fluorophore, so that the standard deviations σ_{x_c} of the standard are negligible compared to σ_x, for comparable measuring times and counting rates. Usually, n was a few channels before the maximum of the fluorescence intensity and $n' = 480$. In a few cases, such as the study of fluorescence standards, n was in one of the first few channels so that the fit covered the whole range of the response function (Cross and Fleming 1984).

In fitting the total intensity, an additional parameter was introduced, namely the shift Q between the time axes of the fluorescence intensity $s(t)$ and the response function $p(t)$ or the fluorescence standard intensity $s_c(t)$. For measurements employing a fluorescence standard this shift should be small and typically is smaller than one channel, whereas for measurements employing the response function the shift may be larger (Lampert et al. 1983). The Q value obtained from the fit of the total intensity is used for the fit of the anisotropy.

If the anisotropy is fitted by adopting the theory of rotational diffusion in an ordering potential (see next paragraph), the unknown parameters to be determined from the fit are the angles of the absorption and emission dipole moments relative to the long molecular axis, the diffusion coefficients for rotation about the long and short molecular axes, and the order parameters $\langle P_2\rangle$ and $\langle P_4\rangle$.

Theoretical description of FAD

Assuming that the probe molecules are symmetric ellipsoids which undergo rotational diffusion in an ordering potential, the fluorescence anisotropy is within good approximation given by an expression like Eq. (3) with 9 exponential terms (van der Meer et al. 1984)

$$R(t) = \tfrac{2}{5}[g_0(\beta_{00}e^{-t/\phi_{00}} + 2\beta_{10}e^{-t/\phi_{10}} + 2\beta_{20}e^{-t/\phi_{20}} + \langle P_2\rangle^2) + g_1(\beta_{01}e^{-t/\phi_{01}} + 2\beta_{11}e^{-t/\phi_{11}} + 2\beta_{21}e^{-t/\phi_{21}}) + g_2(\beta_{02}e^{-t/\phi_{02}} + 2\beta_{12}e^{-t/\phi_{12}} + 2\beta_{22}e^{-t/\phi_{22}})] \tag{11}$$

with the coefficients

$$g_0 = \tfrac{1}{4}(3\cos^2\theta_a - 1)(3\cos^2\theta_e - 1)$$

$$g_1 = 3\sin\theta_a\cos\theta_a\sin\theta_e\cos\theta_e$$

$$g_2 = \tfrac{3}{4}\sin^2\theta_a\sin^2\theta_e$$

$$\beta_{00} = \tfrac{1}{5} + \tfrac{2}{7}\langle P_2\rangle + \tfrac{18}{35}\langle P_4\rangle - \langle P_2\rangle^2$$
$$\beta_{10} = \tfrac{1}{5} + \tfrac{1}{7}\langle P_2\rangle - \tfrac{12}{35}\langle P_4\rangle = \beta_{01}$$
$$\beta_{20} = \tfrac{1}{5} - \tfrac{2}{7}\langle P_2\rangle + \tfrac{3}{35}\langle P_4\rangle = \beta_{02}$$
$$\beta_{11} = \tfrac{1}{5} + \tfrac{1}{14}\langle P_2\rangle + \tfrac{8}{35}\langle P_4\rangle$$
$$\beta_{21} = \tfrac{1}{5} - \tfrac{1}{7}\langle P_2\rangle - \tfrac{2}{35}\langle P_4\rangle = \beta_{12}$$
$$\beta_{22} = \tfrac{1}{5} + \tfrac{2}{7}\langle P_2\rangle + \tfrac{1}{70}\langle P_4\rangle \qquad (12)$$

and the relaxation times

$$\phi_{00}^{-1} = 6D_\perp(\tfrac{1}{5} + \tfrac{1}{7}\langle P_2\rangle - \tfrac{12}{35}\langle P_4\rangle)\,\beta_{00}^{-1}$$
$$\phi_{10}^{-1} = 6D_\perp(\tfrac{1}{5} + \tfrac{1}{14}\langle P_2\rangle + \tfrac{8}{35}\langle P_4\rangle)\,\beta_{10}^{-1}$$
$$\phi_{20}^{-1} = 6D_\perp(\tfrac{1}{5} - \tfrac{1}{7}\langle P_2\rangle - \tfrac{2}{35}\langle P_4\rangle)\,\beta_{20}^{-1}$$
$$\phi_{01}^{-1} = D_\perp(1 + \tfrac{2}{7}\langle P_2\rangle + \tfrac{12}{7}\langle P_4\rangle)\,\beta_{01}^{-1} + D_\parallel$$
$$\phi_{11}^{-1} = D_\perp(1 + \tfrac{1}{7}\langle P_2\rangle - \tfrac{8}{7}\langle P_4\rangle)\,\beta_{11}^{-1} + D_\parallel$$
$$\phi_{21}^{-1} = D_\perp(1 - \tfrac{2}{7}\langle P_2\rangle + \tfrac{2}{7}\langle P_4\rangle)\,\beta_{21}^{-1} + D_\parallel$$
$$\phi_{02}^{-1} = D_\perp(\tfrac{2}{5} + \tfrac{2}{7}\langle P_2\rangle - \tfrac{24}{35}\langle P_4\rangle)\,\beta_{02}^{-1} + 4D_\parallel$$
$$\phi_{12}^{-1} = D_\perp(\tfrac{2}{5} + \tfrac{1}{7}\langle P_2\rangle + \tfrac{16}{35}\langle P_4\rangle)\,\beta_{12}^{-1} + 4D_\parallel$$
$$\phi_{22}^{-1} = D_\perp(\tfrac{2}{5} - \tfrac{2}{7}\langle P_2\rangle - \tfrac{4}{35}\langle P_4\rangle)\,\beta_{22}^{-1} + 4D_\parallel . \qquad (13)$$

Here, θ_a and θ_e are the angles of the absorption and emission dipole moments relative to the long molecular axis, $D_\parallel$ and $D_\perp$ are the coefficients of rotational diffusion about axes parallel and perpendicular to the long molecular axis and $\langle P_2\rangle$ and $\langle P_4\rangle$ are orientational order parameters. They are defined as averages of the Legendre polynomials

$$P_2(\cos\beta) = (3\cos^2\beta - 1)/2 \quad \text{and}$$
$$P_4(\cos\beta) = (35\cos^4\beta - 30\cos^2\beta + 3)/8$$

over the angular distribution $p(\beta)$

$$\langle P_{2,4}\rangle = \int_0^\pi P_{2,4}(\cos\beta)\,p(\beta)\sin\beta\,\mathrm{d}\beta . \qquad (14)$$

β denotes the angle between the long axis of an individual molecule and the preferred axis of orientation, usually the membrane normal. For $t=0$ and $t\to\infty$, the anisotropy $R(t)$ reduces to the well-known expressions (Szabo 1980)

$$R_0 = \tfrac{2}{5}P_2(\cos(\theta_a - \theta_e))$$
$$R_\infty = \tfrac{2}{5}P_2(\cos\theta_a)\,P_2(\cos\theta_e)\,\langle P_2\rangle^2 . \qquad (15)$$

Whenever $\theta_a = \theta_e$, one obtains $R_0 = 0.4$.

It is also instructive to consider the two limiting cases of vanishing orientational order, i.e. $\langle P_{2,4}\rangle = 0$, and of infinitely strong order, i.e. $\langle P_{2,4}\rangle = 1$. In the first case, Eq. (11) reduces to

$$R(t) = \tfrac{2}{5}[g_0\,\mathrm{e}^{-6D_\perp t} + g_1\,\mathrm{e}^{-(5D_\perp + D_\parallel)t} + g_2\,\mathrm{e}^{-(2D_\perp + 4D_\parallel)t}]. \qquad (16)$$

This expression is valid for a symmetrical ellipsoid rotating in an isotropic medium and has already been derived previously (Tao 1969). In the second case, Eq. (11) becomes

$$R(t) = \tfrac{2}{5}[g_0 + g_1\,\mathrm{e}^{-D_\parallel t} + g_2\,\mathrm{e}^{-4D_\parallel t}]. \qquad (17)$$

This relation is also obtained from Eq. (16) under the assumption $D_\perp = 0$. This assumption is commonly adopted to describe the rotational diffusion of proteins in membranes (Rigler and Ehrenberg 1973).

The order parameters may be used to derive an approximate form of the distribution function $p(\beta)$. If $\langle P_2\rangle$ and $\langle P_4\rangle$ are known, the best approximation to the true distribution is given by (Pottel et al. 1986)

$$p(\beta) = \frac{1}{N}\exp[c_2 P_2(\beta) + c_4 P_4(\beta)]. \qquad (18)$$

The normalization constant N is determined from the condition $\int_0^\pi p(\beta)\sin\beta\,\mathrm{d}\beta = 1$, and the parameters c_2 and c_4 from the values of $\langle P_2\rangle$ and $\langle P_4\rangle$.

The diffusion coefficients may be further evaluated for the size and shape of the probe molecules if the viscosity η of the surrounding medium is known, or for the viscosity if the geometry of the probe molecules is known. For symmetrical ellipsoids with a large axial ratio $v = a/b \gg 1$, the following relations have been derived (Memming 1961)

$$D_\parallel = \frac{3\,\mathrm{kT}}{16\pi\eta a^3}(v^2 - \ln 2v) \qquad (19\,\mathrm{a})$$

$$D_\perp = \frac{3\,\mathrm{kT}}{16\pi\eta a^3}(2\ln 2v - 1). \qquad (19\,\mathrm{b})$$

These relations are valid in a strict sense only in an isotropic medium with one viscosity, η. They may, however, be applied to membranes in a approximate way by replacing η by $\eta_\parallel$ and $\eta_\perp$ in the expressions for $D_\parallel$ and $D_\perp$.

Results

Fluorescence standards

As a test for the analysis of fluorescence decays the total intensities of BBO and NPN were investigated which both are known to be mono-exponential (Berlman 1971; Matayoshi and Kleinfeld 1981). The excitation and emission wavelengths were $\lambda_{ex} = 335$ nm and $\lambda_{em} = 430$ nm in both cases. If the data for BBO were deconvoluted using the apparatus response function measured at $\lambda_{ex} = \lambda_{em} = 335$ nm and fitted by a mono-exponential decay, we ob-

tained for the fluorescence lifetime $\tau = 1.00$ ns at a $\chi_s^2 = 1.6$ and a time shift between the response function and the fluorescence intensity of $Q = 90$ ps. This large shift is caused mainly by the wavelength dependence of the photomultiplier response which comes into play because the response function was recorded at $\lambda_{em} = 335$ nm and the fluorescence intensity at $\lambda_{em} = 430$ nm (Lampert et al. 1983). The lifetime of BBO was found to be independent of the emission wavelength and the temperature. Upon degassing the sample, the lifetime of BBO increased to $\tau = 1.04$ ns. This value can be compared with the literature value $\tau = 1.15$ ns (Berlman 1971).[1]

For NPN in undegassed cyclohexane, we obtained by the same procedure $\tau = 3.7$ ns at 35 °C and $\tau = 3.9$ ns at 20 °C, independent of the emission wavelength. Here the literature value is $\tau = 4.0$ ns for NPN in degassed benzene at 20 °C (Matayoshi and Kleinfeld 1981).

As a test for data analysis employing a fluorescence standard we evaluated the NPN fluorescence considering BBO as standard with $\tau_s = 1.00$ ns. The NPN fluorescence was again fitted by a mono-exponential decay. For the lifetime we obtained $\tau = 3.7$ ns at $\chi_s^2 = 1.1$, in agreement with the above analysis using the apparatus response function. The time shift was $Q = 13$ ps representing a typical value for the analysis employing a fluorescence standard.

If, conversely, NPN is considered as fluorescence standard with $\tau_s = 3.72$ ns for the evaluation of the BBO intensity, a mono-exponential fit leads to large residuals and $\chi_s^2 = 94$. No improvement is found from a double-exponential fit. The reason for the large residuals lies in the neglect of the statistical error of the fluorescence standard which is not permitted if $\tau_s > \tau$ as in the present case. The lifetime of BBO resulted as $\tau = 1.00$ ns, again in agreement with the above analysis using the response function.

Anisotropies in glycerol and paraffin

To determine the initial anisotropies, r_0, of the different probes, anisotropy measurements of the probes dissolved in glycerol were performed. Figure 2 shows the anisotropy, $r(t)$, of DPH in glycerol at 20 °C, indicating that the probe is relatively immobile. The fit parameters of $s(t)$ and $r(t)$ with $r(t)$ fitted by a mono-exponential decay are summarized in Table 1, together with the data for the other probes TMA-DPH, DPO, and tPnA.

The result for DPH, $r_0 = 0.385$, is similar to the value 0.392 of Kawato et al. (1977). For TMA-DPH, we obtained $r_0 = 0.385$; Prendergast et al. (1981) found 0.39. The lowest value of $r_0 = 0.375$ was obtained for DPO, the highest value of $r_0 = 0.40$ for tPnA, for which Wolber and Hudson (1981) found 0.39. If the anisotropy data are fitted by Eq. (16) for

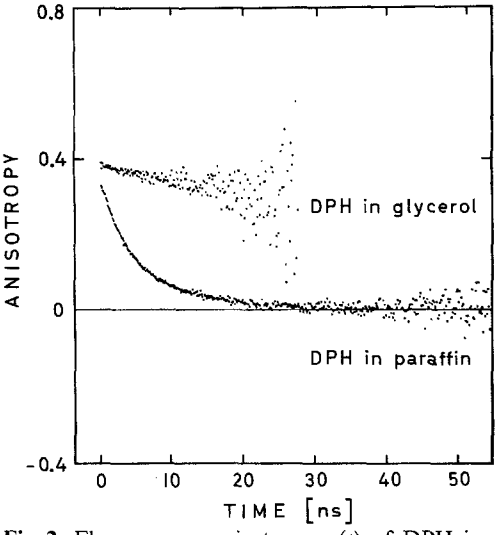

Fig. 2. Fluorescence anisotropy $r(t)$ of DPH in glycerol and paraffin at 20 °C. The results of the fits are presented in Tables 1 and 2

Table 1. Fit parameters for the total intensity and anisotropy of DPH, DPO, TMA-DPH, and tPnA in glycerol. Error limits for all numbers in one line are given at the end of the line

	DPH	DPO	TMA-DPH	tPnA	
Concentration [μM]	4	8	5	2.5	
Temperature [°C]	20	20	20	5	
Standard	BBO	NPN	NPN	BBO	
χ_s^2	1.4	2.4	55[a]	1.3	
τ_1 [ns]	1.5	1.1	1.1	1.0	± 0.2
α_1	0.23	0.82		0.55	± 0.02
τ_2 [ns]	4.0	6.2		3.8	± 0.2
α_2	0.77	0.18		0.45	± 0.02
$\bar{\tau}$ [ns]	3.4	2.0		2.3	± 0.2
χ_d^2	1.7	1.5	18	1.1	
ϕ [ns]	80	80	110	250	± 10
$b = r_0$	0.385	0.375	0.385	0.400	± 0.020

[a] The large value of χ_s^2 is a consequence of the use of NPN as standard which implies $\tau_s \gg \tau$

1 Recently, using rhodamine 6G in the dye laser the fluorescence standard para-terphenyl (PTP) was investigated at $\lambda_{ex} = 290$ nm and $\lambda_{em} = 340$ nm. The lifetime of PTP in undegassed cyclohexane at 20 °C was obtained as $\tau = 0.95$ ns, which upon degassing increased to $\tau = 0.99$ ns. The time shift between the response function and fluorescence intensity was $Q = 40$ ps. The value for τ coincides with the literature value $\tau = 0.99$ ns (Berlman 1971; Wijnaendts van Resandt et al. 1982)

rotational diffusion of a symmetric ellipsoid in an isotropic medium, one obtains for the angles θ_a and θ_e of the absorption and emission dipole moments relative to the long molecular axis $\theta_a = \theta_e$, or $r_0 = 0.4$ according to Eq. (15).

As a test for the analysis of anisotropy decays the anisotropy $r(t)$ of DPH in paraffin at 20 °C was investigated. The data for $r(t)$ are shown in Fig. 2 and the result of the evaluation is presented in Table 2. The time course of $r(t)$ could be fitted reasonably well by a mono-exponential decay. A double-exponential fit yielded a slightly smaller χ_d^2, but the fit parameters were less reproducible in different measurements. For the anisotropy at long times we always obtained $r_\infty = 0$, as expected for orientational fluctuations in an isotropic medium, and for the initial anisotropy $r_0 = 0.35$, a value slightly lower than that determined in glycerol. This result, like the whole set of amplitudes and relaxation times obtained, is in good agreement with the study by Dale et al. (1977).

Adopting the theory for rotational diffusion of a symmetrical ellipsoid in an isotropic medium to DPH in paraffin, the data may be fitted using Eq. (16) (Barkley et al. 1981). From such an analysis one obtains for the angles θ_a and θ_e of the dipole moments and for the coefficients $D_\parallel$ and $D_\perp$ for rotational diffusion about axes parallel and perpendicular to the long molecular axis the values included in Table 2. The dipole moments of DPH are found to be inclined by about 15° relative to the long molecular axis. A CPK model indeed shows that the polyene segment is tilted at an angle of 12° to the long molecular axis going through the centres of the two phenyl rings. Because the dipole moments are oriented nearly parallel to the long molecular axis, the determination of $D_\parallel$ is limited in its precision. If, nevertheless, one uses the values obtained for $D_\parallel$ and $D_\perp$ together with the viscosity of the paraffin employed which was determined as 1.6 p at 20 °C, Eqs. (19) yield for the long and short axes of the DPH molecules $2a = 13.0$ Å and $2b = 1.7$ Å. These values agree fairly well with the numbers 14.3 Å and 2.4 Å derived from molecular orbital calculations (Cehelnik et al. 1974).

Table 2. Fit parameters for the anisotropy of DPH in paraffin at 20 °C. This measurement was performed at $\lambda_{ex} = 315$ nm and the apparatus response function was used for data analysis

χ_d^2	1.2	
ϕ_1 [ns]	2.2	± 0.2
b_1	0.09	± 0.02
ϕ_2 [ns]	6.5	± 0.4
b_2	0.26	± 0.02
$\theta_a = \theta_e$ [deg]	15	± 5
$D \rightarrow D_\parallel$ [μs^{-1}]	326	± 60
$D \rightarrow D_\perp$ [μs^{-1}]	25	± 5

Anisotropies in lipid bilayers

The data for the total intensity, s, and the anisotropy, r, of the four probes in bilayers of DMPC at 35 °C are shown in Fig. 3. For all four probes, the total intensity cannot be described satisfactorily by a mono-exponential decay and, therefore, was fitted by a double-exponential decay. The fitted curves are included in Fig. 3 and the fit parameters are listed in Table 3. For DPH and DPO, the fit by a double-exponential decay is good as expressed by the residuals and $\chi_s^2 < 2$, for TMA-DPH and tPnA the fits are still not optimal.

The anisotropy data for all four probes were fitted first by a mono-exponential relaxation plus a residual anisotropy r_∞. The fit parameters are presented in Table 3. The values obtained for the initial anisotropy r_0 are too small compared with the values obtained in glycerol. If the data were fitted by a double-exponential relaxation, the values for χ_d^2 are lower and the r_0 values closer to those in

Table 3. Fit parameters for the total fluorescence and anisotropy of DPH, DPO, TMA-DPH, and tPnA in bilayers of DMPC at 35 °C

	DPH	DPO	TMA-DPH	tPnA	
χ_s^2	1.9	1.4	3.5	4.8	
τ_1 [ns]	1.8	4.0	0.9	1.2	± 0.2
α_1	0.13	0.12	0.20	0.41	± 0.02
τ_2 [ns]	8.3	6.9	4.1	4.3	± 0.2
α_2	0.87	0.88	0.80	0.59	± 0.02
$\bar{\tau}$ [ns]	7.4	6.6	3.4	3.0	± 0.2
χ_d^2	3.3	1.4	3.8	2.5	
ϕ [ns]	1.4	2.7	1.5	0.9	± 0.2
b	0.261	0.263	0.202	0.210	± 0.02
r_∞	0.046	0.050	0.149	0.087	± 0.01
r_0	0.307	0.313	0.351	0.297	± 0.025
χ_d^2	1.4	1.1	2.1	1.5	
ϕ_1 [ns]	0.33	1.9	0.13	0.30	± 0.2
b_1	0.161	0.194	0.115	0.177	± 0.02
ϕ_2 [ns]	2.2	6.3	2.0	2.6	± 0.3
b_2	0.177	0.088	0.174	0.101	± 0.03
$\bar{\phi}$ [ns]	1.31	3.27	1.26	1.14	± 0.2
r_∞	0.043	0.041	0.142	0.072	± 0.01
r_0	0.381	0.323	0.431	0.350	± 0.035
χ_d^2	1.0	1.6	1.8	2.1	
$\theta_a = \theta_e$ [deg]	11	6	0	0	± 2
$D_\parallel$ [μs^{-1}]	∞	∞	–	–	
$D_\perp$ [μs^{-1}]	203 ± 40	171 ± 60	175 ± 35	909 ± 200	
$\langle P_2 \rangle$	0.342	0.318	0.581	0.459	± 0.015
$\langle P_4 \rangle$	0.378	0.461	0.545	0.583	± 0.060

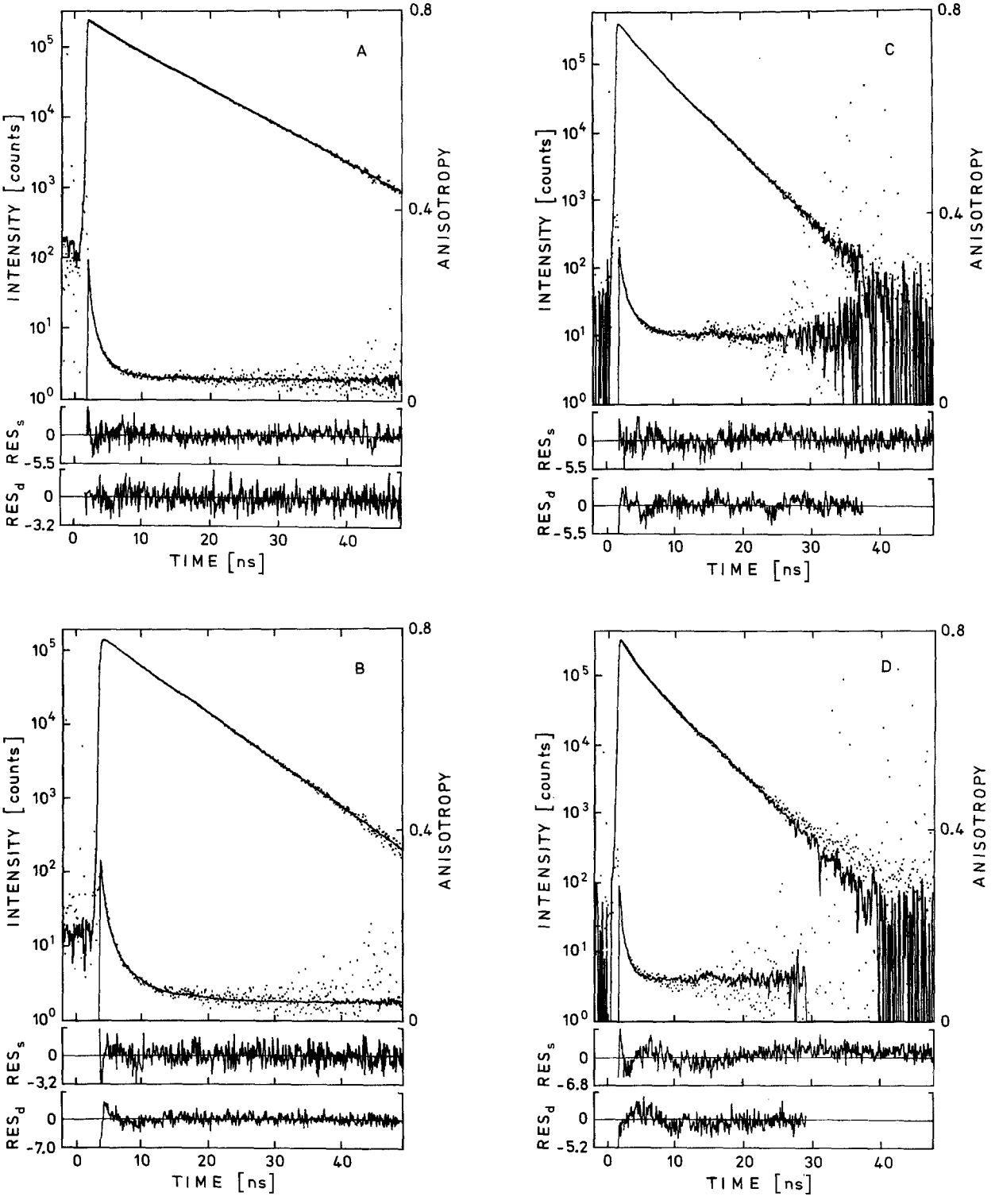

Fig. 3A–D. Total fluorescence intensity $s(t)$ and anisotropy $r(t)$ of DPH (**A**), DPO (**B**), TMA-DPH (**C**), and tPnA (**D**) in bilayers of DMPC at 35 °C. The experimental data are shown (···) together with fitted curves (——) and the corresponding residuals (*lower parts*). The total intensity was fitted by a double-exponential decay and the anisotropy by the theoretical expression Eq. (11). The results of the fits are presented in Table 3

glycerol. Finally, the anisotropy data were fitted by adopting the theoretical expression Eq. (11) for rotational diffusion of symmetric ellipsoids in an ordering potential (van der Meer et al. 1984). The fitted curves and the residuals are included in Fig. 3 and the fit parameters in Table 3. In two cases, that of DPH and TMA-DPH, the fits are better than for double-exponential relaxation, as expressed in lower values of χ_d^2, in the two other cases they are worse. The values obtained for the angles of the absorption and emission dipole moments relative to the long molecular axis are either small, as for DPH and DPO, or zero, as for TMA-DPH and tPnA. As evident from Eqs. (11)–(13), for vanishing θ_a or θ_e the rotational diffusion coefficient $D_\parallel$ cannot be determined. In the two other cases of DPH and DPO, $D_\parallel$ was obtained as $> 10^8\,\mu s^{-1}$ and therefore was fixed at ∞. This implies that for all four probes the anisotropy is described by a triple-exponential relaxation. As an example, for DPH the 3 relaxation times are $\phi_{00} = 2.77$ ns, $\phi_{10} = 0.13$ ns, and $\phi_{20} = 0.63$ ns with the relative amplitudes $\beta_{00} = 0.43$, $\beta_{10} = 0.17$, and $\beta_{20} = 0.29$.

The values for the order parameter $\langle P_2 \rangle$ decrease in the order TMA-DPH > tPnA > DPH > DPO. The values for $\langle P_4 \rangle$ are larger than the $\langle P_2 \rangle$ values for all probes except TMA-DPH where $\langle P_4 \rangle$ is slightly smaller than $\langle P_2 \rangle$. For the two cases of DPH and TMA-DPH, the approximate angular distributions $p(\beta) = (1/N) \exp[c_2 P_2(\beta) + c_4 P_4(\beta)]$ according to Eq. (18) are shown in Fig. 4.

FAD measurements on all four probes were performed at different temperatures in the fluid and the ordered phase of DMPC. The anisotropy data were fitted by the expression for rotational diffusion of a symmetric ellipsoid in an ordering potential providing the temperature dependencies of the angles θ_a and θ_e, of the rotational diffusion coefficients $D_\parallel$ and $D_\perp$, and of the order parameters $\langle P_2 \rangle$ and $\langle P_4 \rangle$. The angles θ_a and θ_e remain essentially constant over the whole temperature range investigated, from 15° to 35 °C. For example, for DPH $\theta_a = \theta_e$ varies between 8° and 14°. The sole exception is TMA-DPH for which $\theta_a = \theta_e$ is zero in the fluid phase (Table 3), but becomes 10° in the ordered phase. Whenever $\theta_a = \theta_e$ is finite, i.e. for DPH and DPO at all temperatures and for TMA-DPH in the ordered phase, the diffusion coefficient $D_\parallel$ is immeasurably large. The temperature dependencies of the diffusion coefficient $D_\perp$ and of the order parameters $\langle P_2 \rangle$ and $\langle P_4 \rangle$ are shown in Fig. 5.

For all probes, both $\langle P_2 \rangle$ and $\langle P_4 \rangle$ increase smoothly upon approaching the phase transition from above and adopt values close to 1 in the ordered phase. It should be noted that the $\langle P_4 \rangle$ values are less reliable than the $\langle P_2 \rangle$ values, because

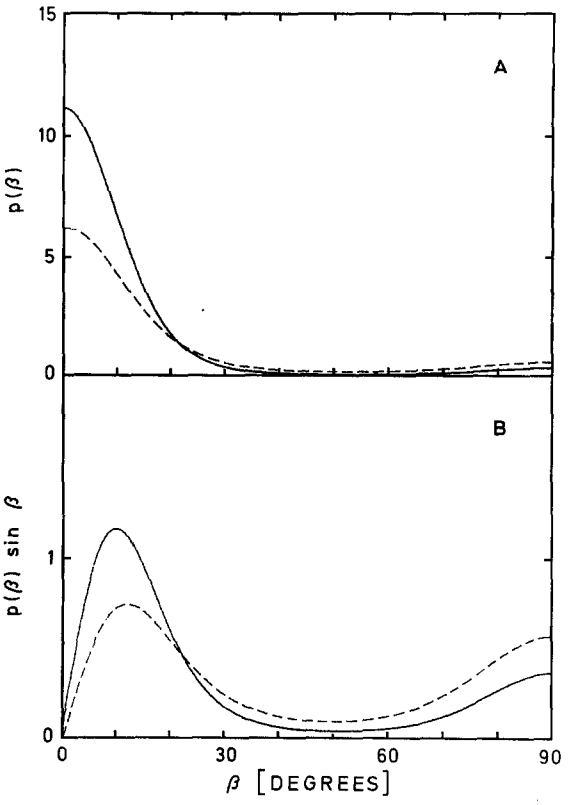

Fig. 4A and B. Approximate angular distributions $p(\beta) = (1/N) \exp[c_2 P_2(\beta) + c_4 P_4(\beta)]$, Eq. (18), for DPH (- - -) and TMA-DPH (——) in fluid membranes of DMPC. The coefficients were determined as $c_2 = 0.55$ and $c_4 = 2.45$ to yield $\langle P_2 \rangle = 0.34$ and $\langle P_4 \rangle = 0.38$ (Table 3) in the case of DPH, and $c_2 = 0.93$, $c_4 = 3.2$ to yield $\langle P_2 \rangle = 0.58$, $\langle P_4 \rangle = 0.55$ for TMA-DPH. The distribution $p(\beta)$ (**A**) and the weighted distribution $p(\beta) \sin\beta$ (**B**) are shown

$\langle P_2 \rangle$ is derived essentially from r_∞ whereas $\langle P_4 \rangle$ follows from the relaxation amplitudes and times. The diffusion coefficients $D_\perp$ of DPH and TMA-DPH behave rather similar. They are more or less constant in the fluid phase – they even seem to increase slightly upon approaching the phase transition, and decrease abruptly at the phase transition. For DPO, $D_\perp$ varies relatively weakly in the whole temperature range investigated. Finally, $D_\perp$ of tPnA seems to decrease at the phase transition as for DPH and TMA-DPH. The error in the $D_\perp$ values of tPnA, however, in considerably larger than for the other probes, because the relaxation of tPnA is much faster and, therefore, more difficult to detect.

Discussion

Orientational order parameter

In this section, we restrict ourselves to a discussion of the order parameter $\langle P_2 \rangle$, postponing a discus-

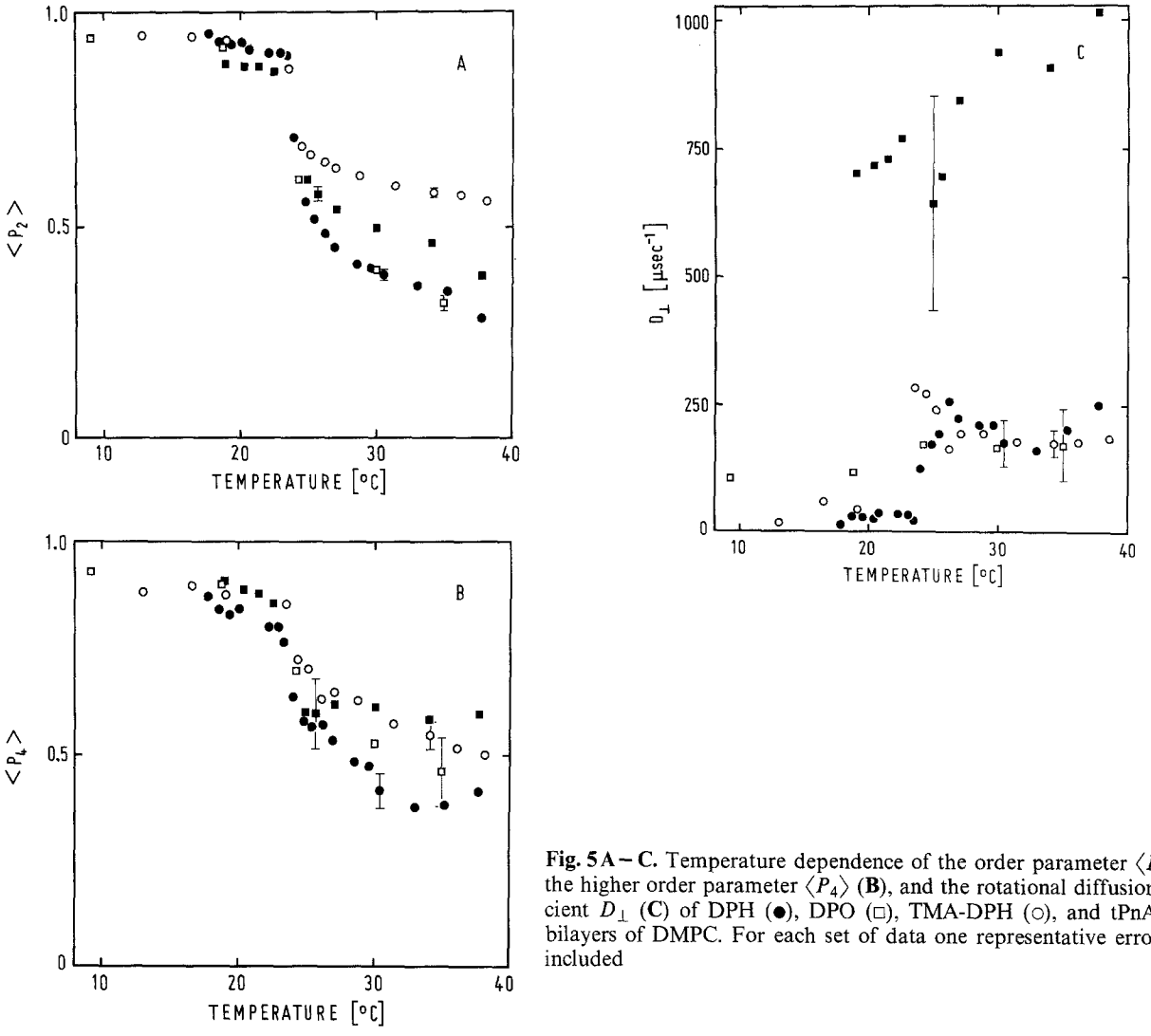

Fig. 5A–C. Temperature dependence of the order parameter $\langle P_2 \rangle$ (**A**), the higher order parameter $\langle P_4 \rangle$ (**B**), and the rotational diffusion coefficient $D_\perp$ (**C**) of DPH (●), DPO (□), TMA-DPH (○), and tPnA (■) in bilayers of DMPC. For each set of data one representative error bar is included

sion of $\langle P_4 \rangle$. The order parameters $\langle P_2 \rangle$ of the four probes in bilayers of DMPC differ, especially in the fluid lipid phase. The reason for this difference must lie either in properties of the probes such as their size, or in differences of their lipid environment. The lipid order parameter $\langle P_2^L \rangle$ is about 0.4 in the so-called plateau region which extends approximately from the carbonyl group to the tenth carbon atom of the chains and then decreases to a value of about 0.2 at the chain ends (Seelig and Seelig 1974). Hence probes at different positions along the membrane normal sense a different lipid environment and, therefore, may differ in their own order. That such an effect exists is borne out by a comparison of TMA-DPH and tPnA. Both probes are expected to insert into a bilayer with their charged ends fixed in the polar head region of the lipids and with the hydrophobic part which carries the fluorophore penetrating between the lipid chains. In the case of TMA-DPH, due to the short connection between the charged moiety and the fluorophore the latter is extended essentially over the plateau region of the lipid chains. tPnA, on the other hand, contains a spacer of 7 CH_2 groups between the charged group and the fluorophore which positions the fluorophore more towards the chain ends. The order parameters are $\langle P_2 \rangle = 0.58$ for TMA-DPH and 0.46 for tPnA (Table 3). The simplest interpretation of this difference is that the fluorophore of tPnA is located deeper in the bilayer where the lipid order is lower. In addition, the fluorophores of TMA-DPH and tPnA differ in size which may also contribute to differences between their order parameters.

To assess the influence of probe size on the order parameter one may compare DPH and DPO. Their positions cannot be as unambiguously fixed as for the charged probes above, but they should not be much different. Therefore, their main difference seems to lie in the size. Since their order parameters are nearly equal, size seems not to have a large effect on probe order.

For a comparison of DPH with the other two probes, one may assume that DPH is located deeper in the membrane than TMA-DPH (Davenport et al. 1985) and, therefore, its order parameter is lower than that of TMA-DPH. Another explanation for the low order parameter of DPH has been given by evoking a partial position of DPH in the middle of the bilayer with an orientation parallel to the membrane plane (Prendergast et al. 1981; Ameloot et al. 1984). This possibility will be discussed in more detail below in connection with the order parameter $\langle P_4 \rangle$. In comparing DPH and tPnA, one might expect that because of similar positions of the two fluorophores in the membrane their order parameters are essentially the same. This seems to be the case for fluid bilayers of DPPC, according to the measurements of Wolber and Hudson (1981). They found for the lipid analogue of tPnA in bilayers of DPPC at 53 °C, i.e. 12 °C above the lipid phase transition, a residual anisotropy of $r_\infty = 0.055$ which yields $\langle P_2 \rangle = 0.37$. This value is close to the DPH order parameter $\langle P_2 \rangle = 0.34$ obtained by us for DMPC at 35 °C, again about 12 °C above the lipid phase transition. The order parameter of tPnA in DMPC at the same temperature, however, is $\langle P_2 \rangle = 0.46$. This might be a consequence of the reduced chain length of DMPC compared to DPPC. Whereas in DPPC the fluorophore of tPnA, like DPH, undergoes normal fluctuations, in DMPC it may dip into the opposite lipid layer which leads to reduced fluctuations and an increased order parameter.

Finally, one can compare probe and lipid order parameters. For this purpose, we choose the probe TMA-DPH which according to the above discussion is the best characterized one. This probe extends over the plateau region of the lipids and its order parameter is $\langle P_2 \rangle \approx 0.6$, much higher than the corresponding lipid order parameter $\langle P_2^L \rangle \approx 0.4$. This difference may be explained in the following manner. Lipid fluctuations as detected by DMR are a superposition of rigid-body motion and conformational transitions, $\langle P_2^L \rangle = \langle P_2^L \rangle_{\text{rigid}} \cdot \langle P_2^L \rangle_{\text{conf}}$ (Petersen and Chan 1977; van der Ploeg and Berendsen 1983; Jähnig et al. 1982). By definition, $\langle P_2^L \rangle_{\text{rigid}}$ does not vary along the lipid chains and the decrease of $\langle P_2^L \rangle$ towards the chain ends is a consequence of increased conformational disorder. A rigid probe extended over the whole length of lipid chains would detect $\langle P_2^L \rangle_{\text{rigid}}$. This also holds, if the probe is confined to the plateau region, whereas a probe located deeper in the bilayer senses an increasing contribution of conformational disorder. Thus, TMA-DPH is expected to reflect only the rigid-body motion of the lipids, $\langle P_2 \rangle = \langle P_2^L \rangle_{\text{rigid}}$. Consequently, its order is higher than the total lipid order as observed. Conversely, this assignment permits a determination of the two components of lipid order. Inserting $\langle P_2^L \rangle \approx 0.4$ and $\langle P_2^L \rangle_{\text{rigid}} \approx 0.6$ into the above relation for $\langle P_2^L \rangle$ yields $\langle P_2^L \rangle_{\text{conf}} \approx 0.6$. Thus, in the plateau region the lipid order originates about equally from rigid-body order and conformational order.

Angular distribution of molecular axes

Complete information on the orientational order of molecules in a membrane would be given by the angular distribution of their long molecular axes and, if necessary, of the short axes. To determine this distribution would require determination of an infinitely larger number of average values such as the order parameters $\langle P_i \rangle$. If only the two order parameters $\langle P_2 \rangle$ and $\langle P_4 \rangle$ are known, the best approximation to the true distribution is given by $p(\beta) \sim \exp[c_2 P_2(\beta) + c_4 P_4(\beta)]$ according to Eq. (18). The approximate distributions derived in this way for DPH and TMA-DPH in fluid bilayers of DMPC (Fig. 4) exhibit a strong maximum at $\beta = 0°$, or at a finite angle β if $p(\beta) \sin\beta$ is plotted, and a weaker maximum at $\beta = 90°$. This would indicate that the probe molecules are oriented preferentially parallel to the membrane normal, with a considerable number of molecules being oriented perpendicular to the membrane normal (Ameloot et al. 1984).

One must, however, be cautious in drawing such a conclusion. The maximum of $p(\beta)$ at $\beta = 90°$ is a consequence of the approximation Eq. (18). The function $P_4(\beta)$ is maximal at $\beta = 90°$, so that whenever the P_4 term in the exponent of $p(\beta)$ dominates over the P_2 term, $p(\beta)$ exhibits a maximum at $\beta = 90°$. If a P_6 term is included in the exponent of $p(\beta)$, one may obtain a minimum of $p(\beta)$ at $\beta = 90°$. An example for such a distribution involving a P_6 term is shown in Fig. 6. However, since only two order parameters have been determined experimentally, the coefficient of the P_6 term cannot be specified.

In addition, a P_1 term in $p(\beta)$ should be included for the following reason. The distributions discussed above are symmetric with respect to $\beta = 90°$. This cannot be correct for asymmetric molecules such as TMA-DPH or lipids, because these molecules sense a potential which orients them with their apolar part into the membrane and not into the water phase. Hence, this potential is asymmetric with respect to $\beta = 90°$ and in the simplest case proportional to P_1 (Jähnig 1979 b; Gruen 1985). Since the potential appears in the exponent of $p(\beta)$, a P_1 term should be included there. An example for a distribution with a P_1 term is also shown in Fig. 6. The height of the maximum or minimum of $p(\beta)$ at

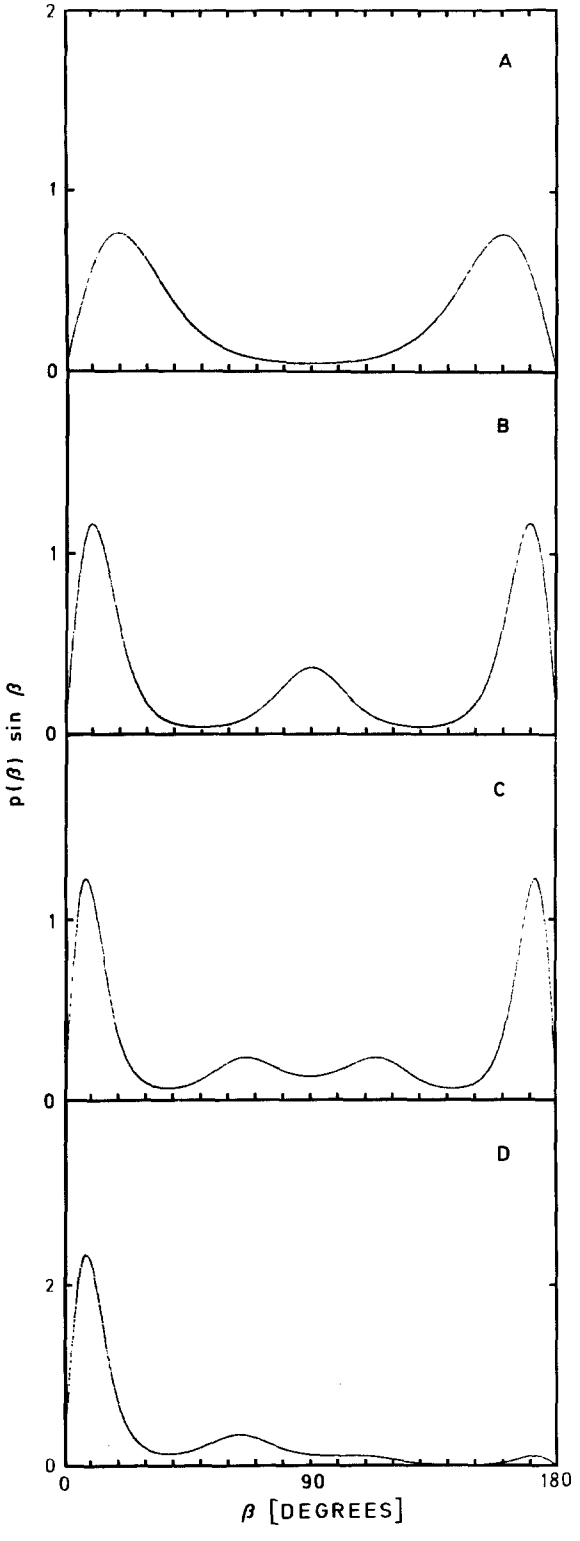

Fig. 6 A–D. Approximate angular distributions $p(\beta) = (1/N) \exp[c_1 P_1(\beta) + c_2 P_2(\beta) + c_4 P_4(\beta) + c_6 P_6(\beta)]$ for TMA-DPH in fluid membranes of DMPC. **(A)** $c_1 = c_4 = c_6 = 0$, $c_2 = 2.8$ yielding $\langle P_2 \rangle = 0.58$, $\langle P_4 \rangle = 0.22$. **(B)** $c_1 = c_6 = 0$, $c_2 = 0.93$, $c_4 = 3.2$ yielding $\langle P_2 \rangle = 0.58$, $\langle P_4 \rangle = 0.55$. **(C)** $c_1 = 0$, $c_2 = 0.9$, $c_4 = 1.4$, $c_6 = 1.9$ yielding $\langle P_2 \rangle = 0.58$, $\langle P_4 \rangle = 0.53$, $\langle P_6 \rangle = 0.50$. **(D)** $c_1 = 1.5$, $c_2 = 0.45$, $c_4 = 1.4$, $c_6 = 1.8$ yielding $\langle P_1 \rangle = 0.69$, $\langle P_2 \rangle = 0.58$, $\langle P_4 \rangle = 0.53$, $\langle P_6 \rangle = 0.46$

$\beta = 90°$ is reduced by the P_1 term. It should be noted that the coefficient of the P_1 term in the distribution can be specified, because the order parameter $\langle P_1 \rangle$ is just the average length of the molecules along the membrane normal. In the case of symmetric probe molecules such as DPH, $p(\beta)$ is symmetric with respect to $\beta = 90°$ and a P_1 term cannot appear.

Although the distribution Eq. (18) involving a P_1 and a P_4 term is the best approximation if only the order parameters $\langle P_2 \rangle$ and $\langle P_4 \rangle$ are known, it is not reliable enough to make definite statements on the true distribution. For TMA-DPH it is evident that the true distribution cannot have a maximum at $\beta = 90°$, in contrast to the approximate distribution. For DPH, there are observations indicating that it behaves in the same way as TMA-DPH. First, the relation between $\langle P_2 \rangle$ and $\langle P_4 \rangle$ is essentially the same for the two probes, as shown in Fig. 7.[2] Second, the relaxation times or diffusion coefficients of both probes are very similar (Table 3 and Fig. 5 C). This suggests that the distribution of DPH is qualitatively similar to that of TMA-DPH. To account for the lower order parameters $\langle P_2 \rangle$ and $\langle P_4 \rangle$ of DPH, its distribution may simply be broader around $\beta = 0$ without becoming maximal at $\beta = 90°$.

Relaxation times

The differences among probe order parameters were attributable predominantly to different positions of the probes along the order parameter profile of lipid order. Since according to DMR relaxation measurements (Brown et al. 1979) the relaxation time of lipid order varies in a similar way along the lipid chains, one might expect that the differences among probe relaxation times can be interpreted in the same way. This would imply that the sequence of probe relaxation times corresponding to their magnitude coincides with the sequence of order parameters. However, this is not the case (Table 3) and another interpretation is required. The most obvious alternative is to explain the differences in relaxation times as differences in probe size: Larger probes diffuse more slowly than smaller ones. DPO is the largest probe, followed by TMA-DPH and DPH, and finally tPnA with the smallest fluorophore. Therefore, the relaxation times should decrease in this order and the diffusion coefficients

2 This result is at variance with the finding of Pottel et al. (1986) who determined $\langle P_2 \rangle$ and $\langle P_4 \rangle$ for TMA-DPH at two different temperatures. Their $\langle P_4 \rangle$ values are much lower than ours

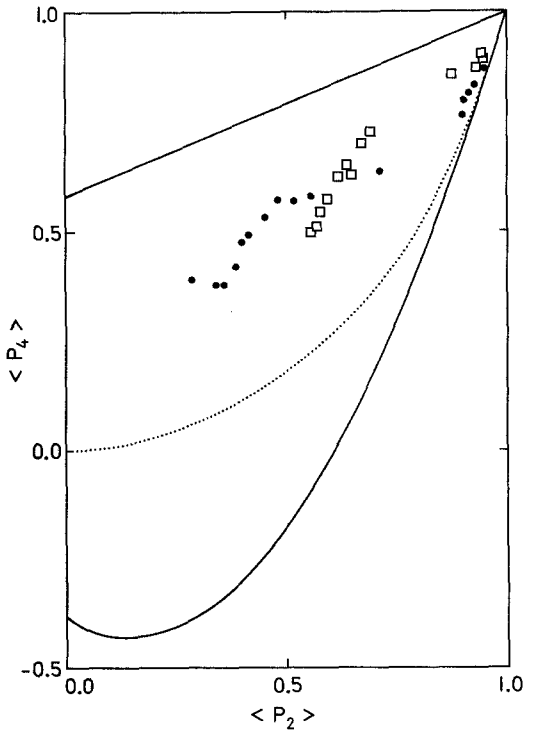

Fig. 7. The relation between the order parameters $\langle P_2 \rangle$ and $\langle P_4 \rangle$ for DPH (●) and TMA-DPH (□) in bilayers of DMPC. The *dotted line* corresponds to the Gaussian distribution $p(\beta) \sim \exp[c_2 P_2(\beta)]$ and the *solid lines* represent the theoretical upper and lower limits for $\langle P_4 \rangle$ according to Kooyman et al. (1981)

increase, as actually found. For tPnA, this interpretation requires that the linkage of the polyene fluorophore to the paraffin chain is highly flexible. This may be the case, because a single bond next to a double bond is relatively flexible.

As discussed above, lipid order is a superposition of rigid-body and conformational order. Correspondingly, lipid relaxation involves two relaxation processes. The conformational order relaxes with a typical times of $\phi^L_{\text{conf}} \approx 0.1$ ns, according to DMR measurements (Brown et al. 1979). Using an ESR probe, the rigid-body order was found to relax with a time of $\phi^L_{\text{rigid}} > 10$ ns (Lange et al. 1985). This relaxation time should be comparable with typical fluorescence probe relaxation times. For all four probes studied, mean relaxation time $\bar{\phi}$ is about 1 ns, hence at least an order of magnitude smaller than the ESR relaxation time. The reason for this difference is unclear.

Diffusion coefficients and viscosities

The ultimate goal in measuring probe relaxation in membranes is to determine the membrane viscosity. This is achieved by evaluating the relaxation times in terms of rotational diffusion coefficients which then can be evaluated for the viscosity.

In all cases where the data could be analyzed for the diffusion coefficient $D_\parallel$ for rotation about the long molecular axis – this is possible only if the absorption and emission dipole moments make a finite angle with the long molecular axis – the diffusion coefficient $D_\parallel$ turned out to be unmeasurably large. Thus, the probe molecules can rotate about their long axes without being hindered by the surrounding lipid molecules. This corresponds to a "slip" boundary condition as opposed to the usual "stick" boundary condition (Hu and Zwanzig 1974). Equivalently, this observation may be expressed by a vanishing viscosity $\eta_\parallel = 0$ for rotation of the probe molecules about an axis parallel to the membrane normal.

The diffusion coefficient $D_\perp$ for rotation about the short molecular axes was finite for all four probes studied. For DPH, its value of $D_\perp = 2 \cdot 10^8 \text{s}^{-1}$ leads, using Eq. (19b), to a viscosity $\eta_\perp = 0.2$ p for rotation or wobbling about an axis perpendicular to the membrane normal.

These results indicate that a membrane cannot be considered as an isotropic medium with one viscosity. Rotation about different axes obey different viscosities: $\eta_\parallel \approx 0$ p and $\eta_\perp = 0.2$ p. The situation becomes even more complicated if larger molecules such as proteins are taken into account. Integral membrane proteins such as bacteriorhodopsin are fixed in a transmembrane orientation so that $D_\perp$ and $\eta_\perp$ cannot be specified, because the ordering potential is too high (Eq. (17)). Rotational diffusion about the fixed axis, however, takes place and the measured diffusion coefficient $D_\parallel$ leads to a viscosity of $\eta_\parallel = 1-4$ p (Cherry and Godfrey 1981; Pauls et al. 1985). Thus, the viscosity $\eta_\parallel$ for protein rotation is finite and an order of magnitude larger than $\eta_\perp$ for wobbling of small probes.

Interestingly, the viscosity η_t for translational motion derived from the lateral diffusion coefficient is also of the order of 1 p. This has been shown for proteins as well as for smaller molecules such as lipids (Peters and Cherry 1982; Vaz et al. 1984). Hence, one may speculate that three viscosities are necessary to characterize the fluidity of a membrane: One viscosity for motions which are connected with positional displacements of lipid molecules – this would include translation and rotation of proteins (Träuble and Eibl 1973) as well as translation of small molecules such as lipids – and another viscosity for motions which are coupled to orientational fluctuations of lipid molecules – this would apply to the wobbling of small molecules. Finally, for motions which are not hindered by lipid mole-

cules such as the rotation of small molecules about their long axis the viscosity vanishes.

Acknowledgements. Thanks are due to several people who helped in setting up the fluorescence apparatus: D. Phillips and D. V. O'Connor from the Faraday Research Laboratory for providing a circuit diagram for the photomultiplier and a computer program for data analysis, G. Marowski from the Max-Planck-Institut für biophysikalische Chemie for help with diodes, H. Reinmuth for constructing the mechanical accessories, and K. Dornmair for his frequent help in case of trouble. We also acknowledge the continuous support and encouragement of P. Overath, and the careful reading of the manuscript by K. Wright.

References

Ameloot M, Hendrickx H, Herreman W, Pottel H, Cauwelaert F van, Meer W van der (1984) Effect of orientational order on the decay of the fluorescence anisotropy in membrane suspensions. Experimental verification on unilamellar vesicles and lipid/α-lactalbumin complexes. Biophys J 46: 525–539

Arcioni A, Zannoni C (1984) Intensity deconvolution in fluorescence depolarization studies of liquids, liquid crystals and membranes. Chem Phys 88:113–128

Barkley MD, Kowalczyk AA, Brand L (1981) Fluorescence decay studies of anisotropic rotations of small molecules. J Chem Phys 75:3581–3593

Berlman I (1971) Handbook of fluorescence spectra of aromatic molecules. Academic Press, New York, p 298

Bevington PR (1969) Data reduction and error analysis for the physical sciences. McGraw-Hill, New York

Brown MF, Seelig J, Häberlen U (1979) Structural dynamics in phospholipid bilayers from deuterium spin-lattice relaxation time measurements. J Chem Phys 70:5045–5053

Cehelnik ED, Cundall RB, Lockwood JR, Palmer TF (1974) Time dependent fluorescence polarization studies using isotropic and liquid crystal media. J Chem Soc Faraday Trans II 70:244–252

Chen LA, Dale RE, Roth S, Brand L (1977) Nanosecond time-dependent fluorescence depolarization of diphenylhexatriene in dimyristoyllecithin vesicles and the determination of "microviscosity". J Biol Chem 252:2163–2169

Cherry RJ, Godfrey RE (1981) Anisotropic rotation of bacteriorhodopsin in lipid membranes. Biophys J 36:257–276

Cross AJ, Fleming GR (1984) Analysis of time-resolved fluorescence anisotropy decays. Biophys J 46:45–56

Dale RE, Chen LA, Brand L (1977) Rotational relaxation of the "microviscosity" probe diphenylhexatriene in paraffin oil and egg lecithin vesicles. J Biol Chem 252:7500–7510

Davenport L, Dale RE, Bisby RH, Cundall RB (1985) Transverse location of the fluorescent probe 1,6-diphenyl-1,3,5-hexatriene in model lipid bilayer membrane systems by resonance excitation energy transfer. Biochemistry 24: 4097–4108

Gruen DWR (1985) A model for the chains in amphiphilic aggregates. 1. Comparison with a molecular dynamics simulation of a bilayer. J Phys Chem 89:146–153

Heyn MP (1979) Determination of lipid order parameters and rotational correlation times from fluorescence depolarization experiments. FEBS Lett 108:359–364

Hu CM, Zwanzig R (1974) Rotational friction coefficients for spheroids with the slipping boundary condition. J Chem Phys 60:4354–4357

Jähnig F (1979a) Structural order of lipids and proteins in membranes: Evaluation of fluorescence anisotropy data. Proc Natl Acad Sci USA 76:6361–6365

Jähnig F (1979b) Molecular theory of lipid membrane order. J Chem Phys 70:3279–3290

Jähnig F, Vogel H, Best L (1982) Unifying description of the effect of membrane proteins on lipid order. Verification for the melittin/dimyristoylphosphatidylcholine system. Biochemistry 21:6790–6798

Kawato S, Kinosita K, Ikegami A (1977) Dynamic structure of lipid bilayers studied by nanosecond fluorescence techniques. Biochemistry 16:2319–2324

Kinosita K, Kawato S, Ikegami A (1977) A theory of fluorescence polarization decay in membranes. Biophys J 20: 289–305

Kinosita K, Kawato S, Ikegami A (1984) Dynamic structure of biological and model membranes: Analysis by optical anisotropy decay measurement. Adv Biophys 17:147–203

Kolber ZS, Barkley MD (1986) Comparison of approaches to the instrumental response function in fluorescence decay measurements. Anal Biochem 152:6–21

Kooyman RPH, Levine YK, Meer W van der (1981) Measurement of second and fourth rank order parameters by fluorescence polarization experiments in a lipid membrane system. Chem Phys 60:317–326

Lakowicz JR, Prendergast F, Hogen D (1979) Differential polarized phase fluorimetric investigations of diphenylhexatriene in lipid bilayers. Quantitation of hindered depolarizing rotations. Biochemistry 18:508–519

Lakowicz JR, Cherek H, Maliwal BP (1985) Time-resolved fluorescence anisotropy of diphenylhexatriene and perylene in solvents and lipid bilayers obtained from multifrequency phase-modulation fluorometry. Biochemistry 24: 376–383

Lampert RA, Chewter LA, Phillips D, O'Connor DV, Roberts AJ, Meech SR (1983) Standards for nanosecond fluorescence decay time measurements. Anal Chem 55:68–73

Lange A, Marsh D, Wassmer KH, Meier P, Kothe G (1985) Electron spin resonance study of phospholipid membranes employing a comprehensive line-shape model. Biochemistry 24:4383–4392

Libertini LJ, Small EW (1984) F/F deconvolution of fluorescence decay data. Anal Biochem 138:314–318

Löfroth JE (1985) Deconvolution of single photon counting data with a reference method and global analysis. Eur Biophys J 13:45–58

Matayoshi ED, Kleinfeld AM (1981) Emission-wavelength-dependent decay of the fluorescent probe *N*-phenyl-1-naphthylamine. Biochim Biophys Acta 644:233–243

Meer W van der, Pottel H, Herreman W, Ameloot M, Hendricks H, Schröder H (1984) Effect of orientational order on the decay of the fluorescence anisotropy in membrane suspensions. A new approximate solution of the rotational diffusion equation. Biophys J 46:515–523

Memming R (1961) Theorie der Fluoreszenzpolarisation für nicht kugelsymmetrische Moleküle. Z Phys Chem 28: 168–189

Pauls KP, MacKay AL, Söderman O, Bloom M, Tanjea AK, Hodges RS (1985) Dynamic properties of the backbone of an integral membrane polypeptide measured by ^{2}H-NMR. Eur Biophys J 12:1–11

Peters R, Cherry RJ (1982) Lateral and rotational diffusion of bacteriorhodopsin in lipid bilayers: Experimental test of the Saffman-Delbrück equations. Proc Natl Acad Sci USA 79:4317–4321

Petersen NO, Chan SI (1977) More on the motional state of lipid bilayer membranes: Interpretation of order param-

eters obtained from nuclear magnetic resonance experiments. Biochemistry 16:2657–2667

Ploeg P van der, Berendsen HJC (1983) Molecular dynamics of a bilayer membrane. Mol Phys 49:233–248

Pottel H, Herreman W, Meer W van der, Ameloot M (1986) On the significance of the fourth-rank orientational order parameter of fluorophores in membranes. Chem Phys 102:37–44

Prendergast FG, Haugland RP, Callahan PJ (1981) 1-[4-(Trimethylamino)phenyl]-6-phenylhexa-1,3,5-triene: Synthesis, fluorescence properties, and use as a fluorescence probe of lipid bilayers. Biochemistry 20:7333–7338

Rigler R, Ehrenberg M (1973) Molecular interactions and structure as analyzed by fluorescence relaxation spectroscopy. Qu Rev Biophys 6:139–199

Robbins RJ, Fleming GR, Beddard GS, Robinson GW, Thistlethwaite PJ, Woolfe GJ (1980) Photophysics of aqueous tryptophan: pH and temperature effects. J Am Chem Soc 102:6271–6279

Seelig A, Seelig J (1974) The dynamic structure of fatty acyl chains in a phospholipid bilayer measured by deuterium magnetic resonance. Biochemistry 13:4839–4845

Szabo A (1980) Theory of polarized fluorescent emission in uniaxial liquid crystals. J Chem Phys 72:4620–4626

Tao T (1969) Time-dependent fluorescence depolarization and Brownian rotational diffusion coefficients of macromolecules. Biopolymers 8:609–632

Thulborn KR, Beddard GS (1982) The effect of cholesterol on the time-resolved emission anisotropy of 12-(9-anthroyloxy) stearic acid in dipalmitoylphosphatidylcholine bilayers. Biochim Biophys Acta 693:246–252

Träuble H, Eibl H (1973) Lipid motion and rhodopsin rotation. Nature 245:210–211

Vaz WLC, Goodsaid-Zalduondo F, Jacobson K (1984) Lateral diffusion of lipids and proteins in bilayer membranes. FEBS Lett 174:199–207

Visser AJWG, Hoek A van (1979) The measurement of subnanosecond fluorescence decay of flavins using time-correlated photon counting and a mode-locked Ar ion laser. J Biochem Biophys Methods 1:195–208

Wahl P (1975) Nanosecond pulsefluorimetry. In: Pain RH, Smith BJ (eds) New techniques in biophysics and cell biology, vol 2. Wiley, London, pp 233–285

Wahl P (1979) Analysis of fluorescence anisotropy decays by a least square method. Biophys Chem 10:91–104

Wahl P, Auchet JC, Donzel B (1974) The wavelength dependence of the response of a pulse fluorimeter using the single photoelectron counting method. Rev Sci Instrum 45:28–32

Wijnaendts van Resandt RW, Maeyer L de (1981) Picosecond rotational diffusion by differential single-photon fluorescence spectroscopy. Chem Phys Lett 78:219–223

Wijnaendts van Resandt RW, Vogel RH, Provencher SW (1982) Double beam fluorescence lifetime spectrometer with subnanosecond resolution: Application to aqueous tryptophan. Rev Sci Instrum 53:1392–1397

Wolber PK, Hudson BS (1981) Fluorescence lifetime and time-resolved polarization anisotropy studies of acyl chain order and dynamics in lipid bilayers. Biochemistry 20: 2800–2810

Zannoni C (1981) A theory of fluorescence depolarization in membranes. Mol Phys 42:1303–1320

Zegel M van den, Boens N, Daems D, Schryver FC de (1986) Possibilities and limitations of the time-correlated single photon counting technique: A comparative study of correction methods for the wavelength dependence of the instrument response function. Chem Phys 101:311–335

Zuker M, Szabo AG, Bramall L, Krajcarski DT, Selinger B (1985) Delta function convolution method (DFCM) for fluorescence decay experiments. Rev Sci Instrum 56:14–22